

See discussions, stats, and author profiles for this publication at: <https://www.researchgate.net/publication/235785503>

# Gene Responses in the Central Nervous System of Zebrafish Embryos Exposed to the Neurotoxicant Methyl Mercury

ARTICLE *in* ENVIRONMENTAL SCIENCE & TECHNOLOGY · MARCH 2013

Impact Factor: 5.33 · DOI: 10.1021/es3050967 · Source: PubMed

CITATIONS

11

READS

157

7 AUTHORS, INCLUDING:



[Lixin Yang](#)

Karlsruhe Institute of Technology

17 PUBLICATIONS 423 CITATIONS

[SEE PROFILE](#)



[Olivier Armant](#)

Karlsruhe Institute of Technology

25 PUBLICATIONS 776 CITATIONS

[SEE PROFILE](#)



[Masanari Takamiya](#)

Karlsruhe Institute of Technology

14 PUBLICATIONS 177 CITATIONS

[SEE PROFILE](#)



[Sepand Rastegar](#)

Karlsruhe Institute of Technology

42 PUBLICATIONS 1,143 CITATIONS

[SEE PROFILE](#)

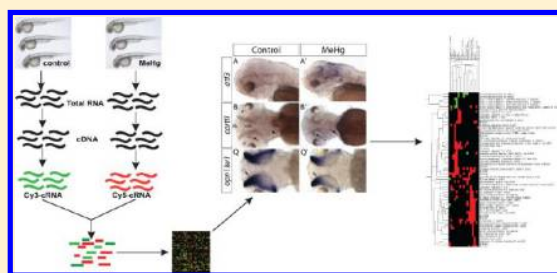
## Gene Responses in the Central Nervous System of Zebra Fish Embryos Exposed to the Neurotoxicant Methyl Mercury

Nga Yu Ho, Lixin Yang, Jessica Legradi, Olivier Armant, Masanari Takamiya, Sepand Rastegar, and Uwe Strahle\*

Institute of Toxicology and Genetics, Karlsruhe Institute of Technology, Hermann-von-Helmholtz-Platz 1, 76344 Eggenstein-Leopoldshafen, Germany

\* Supporting Information

**ABSTRACT:** Methyl mercury (MeHg) is a neurotoxicant with adverse effects on the development of the nervous system from fish to man. Despite a detailed understanding of the molecular mechanisms by which MeHg affects cellular homeostasis, it is still not clear how MeHg causes developmental neurotoxicity. We performed here a genome-wide transcriptional analysis of MeHg-exposed zebra fish embryos and combined this with a whole-mount in situ expression analysis of 88 MeHg-affected genes. The majority of the analyzed genes showed tissue- and region-restricted responses in various organs and tissues. The genes were linked to gene ontology terms like oxidative stress, transport and cell protection. Areas even within the central nervous system (CNS) are affected differently resulting in distinct cellular stress responses. Our study revealed an unexpected heterogeneity in gene responses to MeHg exposure in different tissues and neuronal subregions, even though the known molecular action of MeHg would predict a similar burden of exposed cells. The overall structure of the developing brain of MeHg-exposed embryos appeared normal, suggesting that the mechanism leading to differentiation of the CNS is not overtly affected by exposure to MeHg. We propose that MeHg disturbs the function of the CNS by disturbing the cellular homeostasis. As these cellular stress responses comprise genes that are also involved in normal neuronal activity and learning, MeHg may affect the developing CNS in a subtle manner that manifests itself in behavioral deficits.



### INTRODUCTION

Mercury is a well-known teratogenic and neurotoxin in humans.<sup>1–3</sup> Both natural geological sources, industrial activities and enrichment of mercury and its organic derivatives like methylmercury (MeHg) through the food chain can contribute to human exposure.<sup>4–6</sup> While Hg levels in surface waters, groundwater, and oceans are usually low in the range of 20 ng/L,<sup>7</sup> areas heavily polluted by anthropogenic mercury sources can have MeHg levels of more than 2000 ng/L.<sup>8</sup> The concentration of MeHg can increase by accumulation in the food chain million-fold.<sup>9–11</sup> About 95% of MeHg in the diet is absorbed by the gastrointestinal tract<sup>12</sup> and passes to all main tissues even penetrating the blood-brain barrier.<sup>13,14</sup> MeHg poisoning can result in sensory disturbances, deficits in motor coordination, and somatosensory and psychiatric disorders. The developing human brain is more susceptible to MeHg than the adult brain. Children exposed during pregnancy to subacute doses of MeHg showed impairments in motor coordination, speech and involuntary movement due to damage of the brain, particularly the cerebral and cerebellar cortices.<sup>1–3</sup> After the Minamata poisoning, median hair content of mercury was 30 ppm and the maximum was 920 ppm.<sup>1</sup> The EPA regards 5.8 µg Hg/L blood as safe (<http://www.epa.gov/hg/exposure.htm>). A study of children on the Faroe island suggest that MeHg concentrations below 10 ppm in the hair of the mother

correlate with deficient performance in attention, memory and language of her offspring.<sup>15</sup>

MeHg exposure has been shown to result in various cellular changes such as lipid peroxidation, DNA damage, membrane structure alteration, mitochondrial dysfunction, cell cycle alteration, apoptosis, and necrosis.<sup>16</sup> The interactions with sulfhydryl groups, the induction of oxidative stress and the disruption of calcium ion homeostasis have been reported to be the three major and critical mechanisms.<sup>17–24</sup> It is, however, not clear how MeHg acts as a neurotoxicant. Hence vertebrate models are needed to investigate the neurotoxic effects in detail.

The zebra fish embryo is highly sensitive to MeHg. Exposure of zebra fish embryos to 20 and 30 µg/L MeHg led to impaired development of the caudal fin and caused an abnormal tail exure.<sup>25–27</sup> Doses between 10 and 20 µg/L MeHg induced faint heartbeats, severe edema, upward exures of the body axis, reduced swimming activity, impaired prey capture performance, a delayed mortality syndrome, behavioral deficits<sup>28</sup> and impaired tail formation.<sup>27</sup> Global transcriptome study on zebra fish embryos showed that acute exposure to 60 µg/L

Received: May 30, 2012

Revised: February 28, 2013

Accepted: March 4, 2013



ACS Publications

© XXXX American Chemical Society

A

dx.doi.org/10.1021/es3050967 | Environ. Sci. Technol. XXXX, XXX, XXX–XXX

MeHg induced genes involved in the acute inflammatory response, amino acid metabolism, transmembrane receptor protein tyrosine kinase signaling pathways, and the insulin receptor signaling pathway.<sup>26</sup> Similar transcriptome studies in adult zebra fish indicated that sublethal acute or chronic exposure to MeHg or Hg caused gene expression changes linked to a variety of biological and molecular processes, such as oxidative stress, immune defense, DNA damage, apoptosis, lipid peroxidation, and glycolysis/gluconeogenesis.<sup>29–32</sup> Investigation of the localization of MeHg in adult zebra fish after trophic and chronic MeHg exposure revealed that the brain accumulated high levels of MeHg among the three organs examined.<sup>33</sup> Another study concerning the visual system showed that MeHg could pass through the blood-retina barrier and could accumulate in the retina.<sup>34</sup>

To investigate the mode of action of the neurotoxicant MeHg, we carried out systematic gene expression analysis using zebra fish embryos as models. By a combination of microarray and in situ expression studies, we show that sublethal concentrations of MeHg induce tissue specific gene expression changes in the CNS and in many other organs of the 3-day-old zebra fish embryo. By gene ontology analysis with functions inferred from those of mammalian orthologous genes, most of these genes were linked to cellular stress responses. Our data suggest that MeHg affects neuronal cell homeostasis, thereby affecting the developing brain.

## MATERIALS AND METHODS

**Fish Maintenance and MeHg Treatment.** Zebra fish were maintained and treated with MeHg as described.<sup>26,27</sup> For details see Supporting Information (SI) Material and Methods

**DNA Microarray.** Two-color DNA microarrays (zebra fish gene expression microarray chip 4 × 44K, Agilent Technologies) were hybridized according to the Agilent Low RNA Input Linear Amplification Kit protocol (Agilent Technologies). Three independent repeats were performed for both control and MeHg-treated samples. Two μg total RNA from each sample was reverse transcribed into cDNA (see below). cRNA was transcribed from the cDNA and labeled with Cyanine3 (Cy3) –CTP or Cy5-CTP fluorescent dyes (PerkinElmer/NEN Life Science). The cRNA samples were purified with the RNeasy Mini Kit (Qiagen, Netherlands). Microarray chips were handled according to the user guide of the Agilent Microarray Hybridization Chamber Kit (Agilent Technologies). A dye swap was performed for each biological repeat.

**Data Analysis.** The software MATLAB (version R2010a; Math Works) or the MATLAB toolbox Gait-CAD<sup>35</sup> was modified by adding filtering functions, normalization methods and statistical tests. M-value (Log<sub>2</sub> of fold-change) transformations were performed to obtain a more symmetric distribution of the data. The raw microarray data were preprocessed by background subtraction and normalized by the LOWESS method.<sup>36</sup> Plots of the data distribution of each microarray were examined for control of the quality of hybridizations. The spike controls contained ten in vitro synthesized, polyadenylated transcripts in predetermined ratios for monitoring linearity, sensitivity, and accuracy. The data of the dye swaps were averaged using median. A one-sample *t* test was performed over the three biological replicates to identify statistically significant differences (*p* < 0.05). The M-values of the replicates were averaged (using median). To reduce the false positives, we performed besides the *t* test a M-value cutoff based on the variation of the M values. The false positives had

rather small M-values. The variance of M-values over the replicate was expected to be smaller when arising from a true signal as compared to being caused by noise. To test this, the mean M-values were plotted against the coefficient of variation (CV) over the replicates. A CV value of one was generally used as cutoff between small (CV < 1) and high variance (CV > 1). The M value cutoff was determined by the point where the M-values scattered over the CV of one. Differentially expressed spots (*p*-value < 0.05) with M values greater than 1.4 had a small variance and therefore represented true biological signal. This double filtering method gave a better validation rate.<sup>37</sup> The microarray data were submitted to Gene Expression Omnibus (GEO) with the accession number GSE37970.

**Gene Ontology Analysis.** The regulated genes were assigned to the closest human homologue using BioMart (<http://www.biomart.org/>).<sup>38</sup> The gene ontology (GO) analyses were then carried out with the Gene Set Analysis Toolkit V2 ([http://bioinfo.vanderbilt.edu/wg\\_gsat/](http://bioinfo.vanderbilt.edu/wg_gsat/)).<sup>39,40</sup> Lists of the human homologues were blasted against the human genome. Hypergeometric test, Benjamini & Hochberg (1995) multiple test adjustment (MTC), and a significance level of 0.01 were used for the analysis. Three genes was the minimum number for a category to be determined as enriched.

**Expression Analysis.** In situ hybridization and immunohistochemistry was performed using standard protocols.<sup>41,42</sup> (For details see SI Material and Methods). Tissue annotations of in situ expression data were transformed into a matrix of gene expression (0 no change, 1 upregulated, –1 downregulated) and subjected to hierarchical clustering using the uncentered correlation metric and pairwise average linkage method.<sup>43</sup>

Real-time polymerase chain reaction (RT-qPCR) was carried out following suppliers instructions (For details see SI Material and Methods).

## RESULTS

### Analysis of the Transcriptome of MeHg-Exposed Embryos.

We wished to identify genes whose expression was altered by exposure to MeHg in the developing zebra fish embryo and which might thus serve as reporters of developmental toxicity. Our previous transcriptome analysis<sup>26</sup> of MeHg-treated embryos covered only 10656 probes. We therefore repeated the analysis with the more comprehensive 4 × 44K chip design (Agilent Technologies), which contains 43 803 probes for 13 555 genes (Zebra fish genome assembly, Zv9, v66).

Embryos were exposed from 48 to 72 hpf to 60 μg/L MeHg and changes in gene expression were monitored by comparison with the water control using a two color protocol. Statistical analysis indicated that a total of 464 genes were up-regulated with M-values (log<sub>2</sub> of fold-change) greater than or equal to 1.3 (*p* < 0.05, SI Table S3) and 379 genes were down-regulated with M-values smaller than or equal to –1.3 (*p* < 0.05, SI Table S4).

We analyzed the gene ontology groups to which the MeHg-regulated genes belong with the Gene Set Analysis Toolkit V2 ([http://bioinfo.vanderbilt.edu/wg\\_gsat/](http://bioinfo.vanderbilt.edu/wg_gsat/)).<sup>39,40</sup> One large group of up-regulated genes is involved in apoptosis, and other genes were previously implicated in cell redox homeostasis, oxidative stress, and acute inflammatory responses, suggesting that MeHg caused cell stress and tissue damage. (Table 1, SI Figure 1A, A). Genes encoding phosphatases and endopeptidases were also up-regulated. Several genes involved in other cellular

Table 1. Ontology Groups of Genes Up-Regulated by MeHg

gene ontology	number of genes	adjusted <i>p</i> -value
apoptosis	36	$3.00 \times 10^{-4}$
prostaglandin metabolic process	4	$5.50 \times 10^{-3}$
calcium independent cell–cell adhesion	5	$9.00 \times 10^{-4}$
cell redox homeostasis	6	$5.50 \times 10^{-3}$
response to oxidative stress	12	$3.00 \times 10^{-4}$
acute in ammatory response	8	$2.60 \times 10^{-3}$
blood circulation	12	$2.00 \times 10^{-3}$
MAPKtyrosine/serine/threonin phosphatase activity	4	$4.00 \times 10^{-4}$
endopeptidase activity	19	$1.00 \times 10^{-4}$
serine-type endopeptidase activity	11	$5.00 \times 10^{-4}$
transcription factor activity	26	$6.10 \times 10^{-3}$
aryldialkylphosphatase activity	3	$2.00 \times 10^{-4}$

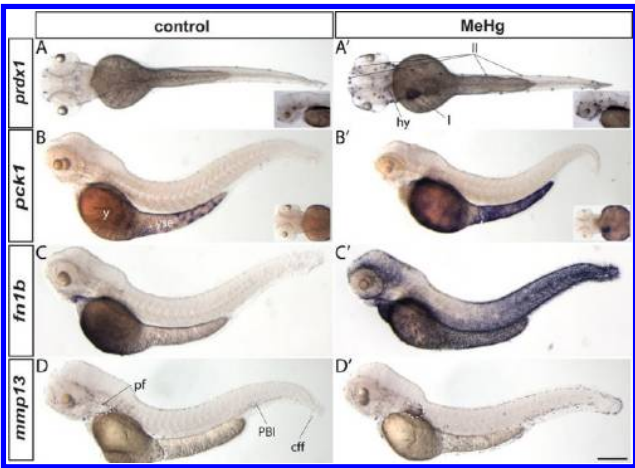
functions were down-regulated by MeHg exposure, such as transcriptional elongation, fatty acid metabolism, DNA repair, and particularly dehydrogenase and isomerase activities (Table 2, SI Figure 1B, B ).

Table 2. Ontology Groups of Genes down-Regulated by MeHg

gene ontology	number of genes	adjusted <i>p</i> -value
RNA elongation from RNA Pol II promoter	6	$3.70 \times 10^{-3}$
fatty acid catabolic process	5	$6.50 \times 10^{-3}$
double strand break repair	6	$5.20 \times 10^{-3}$
transcription factor activity, nucleic acid binding	8	$1.20 \times 10^{-3}$
acyl-CoA binding	4	$1.30 \times 10^{-3}$
3-hydroxyacyl-CoA dehydrogenase activity	3	$1.30 \times 10^{-3}$
peptidyl-prolyl cis–trans isomerase activity	5	$1.50 \times 10^{-3}$

**In Situ Analysis of Expression.** Transcriptome analysis of whole zebra sh embryos does not allow examination of tissue-specific changes in gene expression. In order to verify the microarray data and to derive at the same time information on tissue specific expression of the induced genes, we carried out an in situ expression study with 88 significantly MeHg-regulated genes. Probes were subcloned (SI Table S1) and 72 hpf embryos were subjected to in situ hybridization. Embryos were treated with 60 μg/L MeHg from 4 to 72 hpf and expression patterns were compared to those of water controls. Among the 88 genes analyzed by in situ hybridization, the changes in expression levels of 60 genes were confirmed to be correlated with the microarray results (Figure 1 see also SI Figure 2). For example, *peroxiredoxin1* (*prdx1*) was up-regulated in the lateral line, the liver and the hypothalamus in response to MeHg (Figure 1A, A ). Increased expression of *phosphoenolpyruvate carboxykinase 1* (*pck1*) was observed in the yolk syncytial layer and the liver (Figure 1B, B ); *fibronectin1b* (*fn1b*) showed a strong up-regulation in the skin throughout the whole embryo (Figure 1C, C ). *matrix metalloprotease* (*mmp13*) was up-regulated in cells scattered all over the body, the posterior blood island (PBI), where blood cells are produced, and along the edges of the pectoral and caudal ns (Figure 1D, D ).

**Clustering of Whole-Mount In Situ Hybridizations.** The results derived from the whole-mount in situ hybridizations were classified using the following 17 anatomical terms:



**Figure 1.** Changes in gene expression patterns after MeHg exposure. Control (A, B, C, D) and MeHg-treated (A', B', C', D') embryos (72 hpf) were hybridized with RNA probes complementary to *peroxiredoxin1* (*prdx1*, A, A'), *phosphoenolpyruvate carboxykinase 1* (*pck1*, B, B'), *fibronectin1b* (*fn1b*, C, C') and *matrix metalloprotease13* (*mmp13*, D, D') mRNA. Abbreviations, c, caudal n fold; hy, hypothalamus; l, liver; ll, lateral line; PBI, posterior blood island; pf, pectoral ns; y, yolk; yse, yolk sac extension. Scale bar, A, A' – D, D', 200 μm.

brain, eyes, olfactory bulb, branchial arches, heart, liver, gut, pronephros, somites, lateral line, pectoral ns, caudal n fold, blood vessels, skin, yolk syncytial layer (YSL), pigment cells, and notochord (Figure 2). Three major clusters of coexpressed genes were discernible: *complement factors b*, *3a* and *4–2* are expressed in the YSL and the liver together with *pck1* (Figure 2). Other genes were coexpressed in the brain and the eyes. A third prominent cluster of coexpressed genes was found in the caudal ns and the skin. In 4 cases (*elf3*, *noxo1l*, *cbx7a*, and *slc16a9a*), expression was up-regulated in some tissues and was down-regulated in others (Figure 2). For example, the expression of *noxo1l* was increased in the lateral line, pectoral ns, caudal n fold and skin, but decreased in the branchial arches (SI Figure 2A, A'). Taken together, our results demonstrate that most of the MeHg-regulated genes were expressed in a tissue restricted manner (Figures 1 and 2, SI Figure 2). Different tissues responded with distinct changes in gene expression.

To verify the observed changes in gene expression by an independent method, RT-qPCR was performed with selected genes including *arf4*, *atf3*, *c4–2*, *c6*, *cbx7a*, *homez*, *irf9*, *prdx1*, *ppp1r15a*, *txnl*, *zgc:101661*, and *opn1mw1*. Zebra sh embryos were exposed to 30 or 60 μg/L MeHg from 4 to 72 hpf and cDNA samples were subjected to real-time PCR analysis with gene-specific primers. The expression levels of all the genes examined, except *homez*, were significantly regulated by treatment with 60 μg/L MeHg (Figure 3). In situ hybridization showed that *homez* mRNA was up-regulated in embryos with severe malformations (precordial edema, reduced n folds, smaller brain, curved body), but not in embryos that were morphologically not affected by MeHg treatment. This contributed to variation and thus reduced significance of the RT-qPCR results. *opn1mw1* showed a repression with an M-value of less than –2 after exposure to 60 μg/L MeHg. Down-regulation of other opsin genes was also noted (Figure 2, SI Table S4) suggesting that differentiation of the retina is



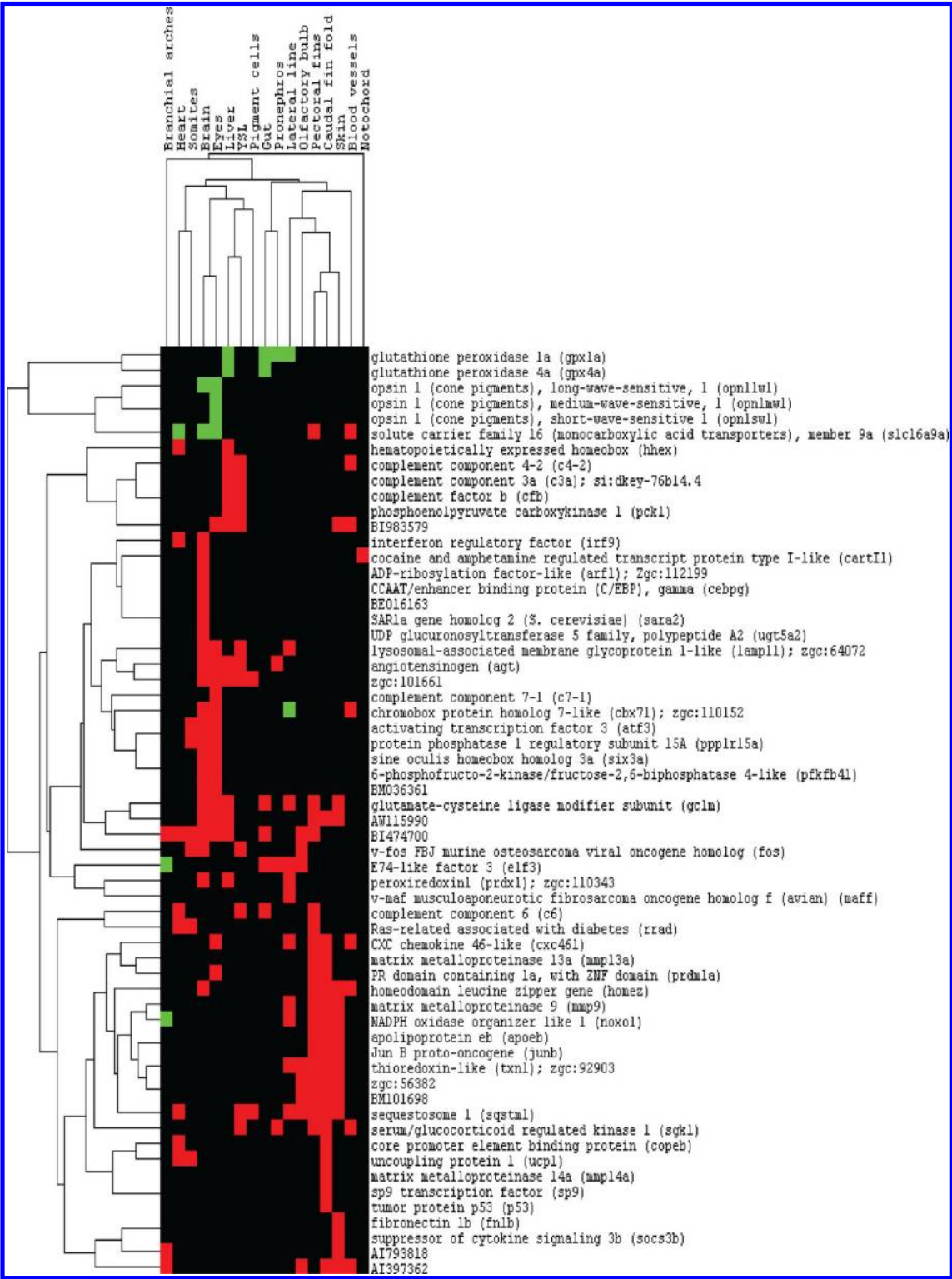


**Figure 2.** Hierarchical clustering of expression patterns of MeHg-regulated genes. The tissues scored are indicated at the top and the gene names are listed on the left. Red, up-regulation; green, down-regulation.

impaired by MeHg. *arf4*, *c4-2*, *c6*, *cbx7a*, *prdx1*, *txnl*, and *zgc:101661* showed significant changes also at 30  $\mu\text{g/L}$  MeHg.

**Genes Showing Ectopic Expression in the Brain of MeHg-Treated Embryos.** MeHg is a known developmental neurotoxicant in humans.<sup>1–3</sup> We therefore focused our attention on MeHg-regulated genes that are expressed in the

CNS of the zebra sh embryo. Among the 88 genes analyzed by in situ hybridization, 24 genes were specifically regulated in the brain in response to MeHg exposure (Figure 2).

The level of mRNA for *activating transcription factor 3* (*atf3*), a leucine zipper transcription factor of the CREB family, was induced in discrete patches in the brain in MeHg-treated

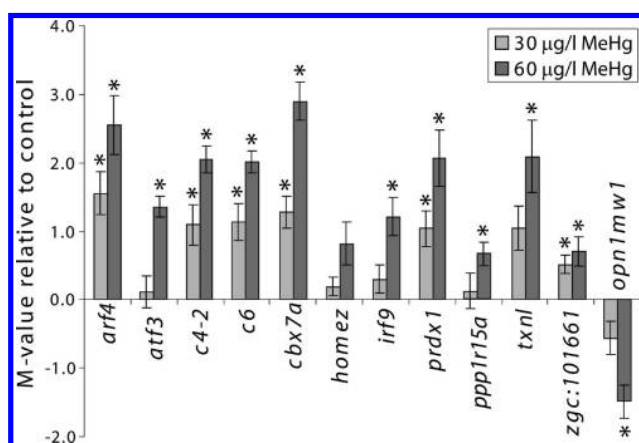


**Figure 3.** Changes in gene expression levels measured by quantitative real-time PCR. The changes in the expression levels of *arf4*, *atf3*, *c4-2*, *c6*, *cbx7a*, *homez*, *irf9*, *prdx1*, *ppp1r15a*, *txnl*, *zgc:101661*, and *opn1mw1* were determined by real-time PCR of cDNA from control and MeHg-treated embryos. Graph of M-value ( $\log_2$  of the fold change) relative to controls against MeHg concentrations is plotted. The mean  $\pm$  SEM are presented. *t* test and Dunnett adjustment, *p* < 0.05 (\*).

embryos (Figure 4A, A). Mammalian ATF3 responds to a wide variety of cellular stresses such as mechanically or toxicant-injured tissues, blood-deprived heart and postseizure brain,<sup>44</sup> and it protects hippocampal neurons from apoptosis.<sup>45</sup> The cocaine and amphetamine regulated transcript protein type I-like (*cart1l*) was weakly expressed in small groups or individual cells located bilaterally in the brain (Figure 4B). The level of *cart1l* transcripts was increased in these cells after MeHg exposure (Figure 4B, B, arrows). Mammalian Cart1 was ascribed a neuroprotective role.<sup>46–48</sup> The Polycomb related *chromobox protein homologue 7a* (*cbx7a*) was induced in an overlapping but different pattern in the brain in MeHg-treated embryos (Figure 4C, C, arrows). The mammalian homologue of *cbx7a* was previously shown to expand the life span of a wide variety of human cells.<sup>49</sup>

The expression of the transcription regulator CCAAT/enhancer binding protein gamma (*cebpg*) was elevated in the dorsal tectum by MeHg treatment (Figure 4D, D). *cebpg* expression was correlated with the expression of antioxidant gene expression in the human lung.<sup>50</sup> The transcription factor FBJ murine osteosarcoma viral oncogene homologue (*fos*) is an immediate early gene responding to cellular stress, growth factors and neuronal activity.<sup>51,52</sup> It was strongly induced in the brain of MeHg-exposed embryos (Figure 4E, E). Also the glutamate-cysteine ligase modifier (*gclm*) showed a general up-regulation in the brain in MeHg-treated embryos with stronger expression in the boundaries between forebrain/midbrain and midbrain/hindbrain and in the dorsal region of the tectum (Figure 4F, F). *Gclm* is a subunit of Glutamate-cysteine ligase, which together with glutathione synthetase maintains high glutathione levels in the cells as a major defense against oxidative stress.<sup>53</sup> Another protein involved in combating oxidative stress is *peroxiredoxin1* (*prdx1*).<sup>54</sup> The expression of *prdx1* was increased in the hypothalamus of the brain of MeHg-treated embryos (Figure 4G, G). The protein phosphatase 1, regulatory subunit 15a (*ppp1r15a*) was detected at higher levels in the tegmentum and rhombomeres of MeHg-treated embryos in comparison to controls (Figure 4H, H). The mammalian

homologue of this gene responds to stressful conditions and its expression is correlated with apoptosis in mammals.<sup>55</sup>

Three developmental genes were also identified to be induced by MeHg treatment. The homeodomain leucine zipper gene (*homez*) was shown to act downstream of proneural genes in the control of neurogenesis in *Xenopus laevis*.<sup>56</sup> It was induced to varying levels in distinct regions throughout the brain by MeHg treatment (Figure 4I, I). However, its ectopic expression was correlated with major malformations of the embryo. While the mRNA of the transcription factor *interferon regulatory factor* (*irf9*) was barely detectable in control embryos, it showed strong expression in the brain of MeHg-treated embryos with stronger expression in the cells lining the ventricles (Figure 4J, J). In contrast to *irf9* and *homez* that showed ectopic expression in the brain, the expression of the homeobox transcription factor *sine oculis homeobox homologue 3a* (*six3a*) was increased in the normal domains of expression in the forebrain (Figure 4K, K). Together, the data from the three developmental genes suggests that MeHg directly or indirectly affects the patterning of the brain and neurogenesis. In addition, we noted that in 60% MeHg-treated embryos (*n* = 3, 30 embryos examined in each experiment) the head was smaller than in controls (for example see Figure 4D, D, SI Figure 6). We thus examined the expression of genes involved in brain patterning including *sonic hedgehog* a (*shha*)<sup>57</sup>, *paired box gene 6a* (*pax6a*)<sup>58</sup>, *bone morphogenetic protein 2b* and 4 (*bmp2b*, *bmp4*)<sup>59</sup>, *fibroblast growth factor 3* and 8 (*fgf3* and *fgf8*)<sup>60,61</sup>, *wingless-type MMTV integration site family, member 1* (*wnt 1*)<sup>62</sup>, *nestin*,<sup>63</sup> *wnt 5b*,<sup>64</sup> and *sox2* (Armant et al, in revision) and *crestin*,<sup>65</sup> and genes involved in neural transmission including *acetylcholinesterase* (*ache*)<sup>66</sup>, *cannabinoid receptor 1* (*cb1*)<sup>67</sup> *serotonin transporter a* (*serta*)<sup>68</sup>, *nuclear receptor-related factor 1* (*nurr1*)<sup>69</sup>, and *tyrosine hydroxylase* (TH<sup>70</sup>). We did not detect significant deviations in the expression of these genes in MeHg-treated embryos relative to the controls (SI Figures 3 and 4). We also assessed whether cilia are affected in MeHg treated embryos by staining with antiacetylated tubulin antibody. Cilia in the pronephros and the inner ear formed normally in MeHg-treated embryos (SI Figure 4I, I, J, J).

A number of affected genes are directly or indirectly involved in transport processes. The expression of *ADP-ribosylation factor 4* (*arf4*) was up-regulated by MeHg in scattered cells in the brain, presumably microglia cells (Figure 4L, L). The GTP binding Arfs belong to the Ras superfamily and are involved in the regulation of membrane traffic and organization of the cytoskeleton.<sup>71</sup> The expression of the vesicular marker *lysosomal-associated membrane glycoprotein 1-like* (*lamp1l*) was elevated especially in the epithelial lining of the brain ventricles (Figure 4M, M). In contrast, the *solute carrier family 16 member 9a* (*slc16a9a*) involved in transport of monocarboxylic acids showed a general decrease in the expression in the brain after MeHg treatment (Figure 4N, N). *UDP glucuronosyltransferase 5, polypeptide A2* (*ugt5a2*) belongs to the phase II detoxifying family of Ugt enzymes that modify compounds by attachment of a glucuronic acid residue to facilitate destruction or secretion.<sup>72</sup> *ugt5a2* was up-regulated in the dorsal region of the brain of MeHg-treated embryos (Figure 4O, O). The *SAR1a gene homologue* (*sara2*), a small GTPase, which is presumed to be involved in transport from the Golgi apparatus,<sup>73</sup> showed moderate up-regulation in the brain of embryos exposed to MeHg (Figure 4P, P).



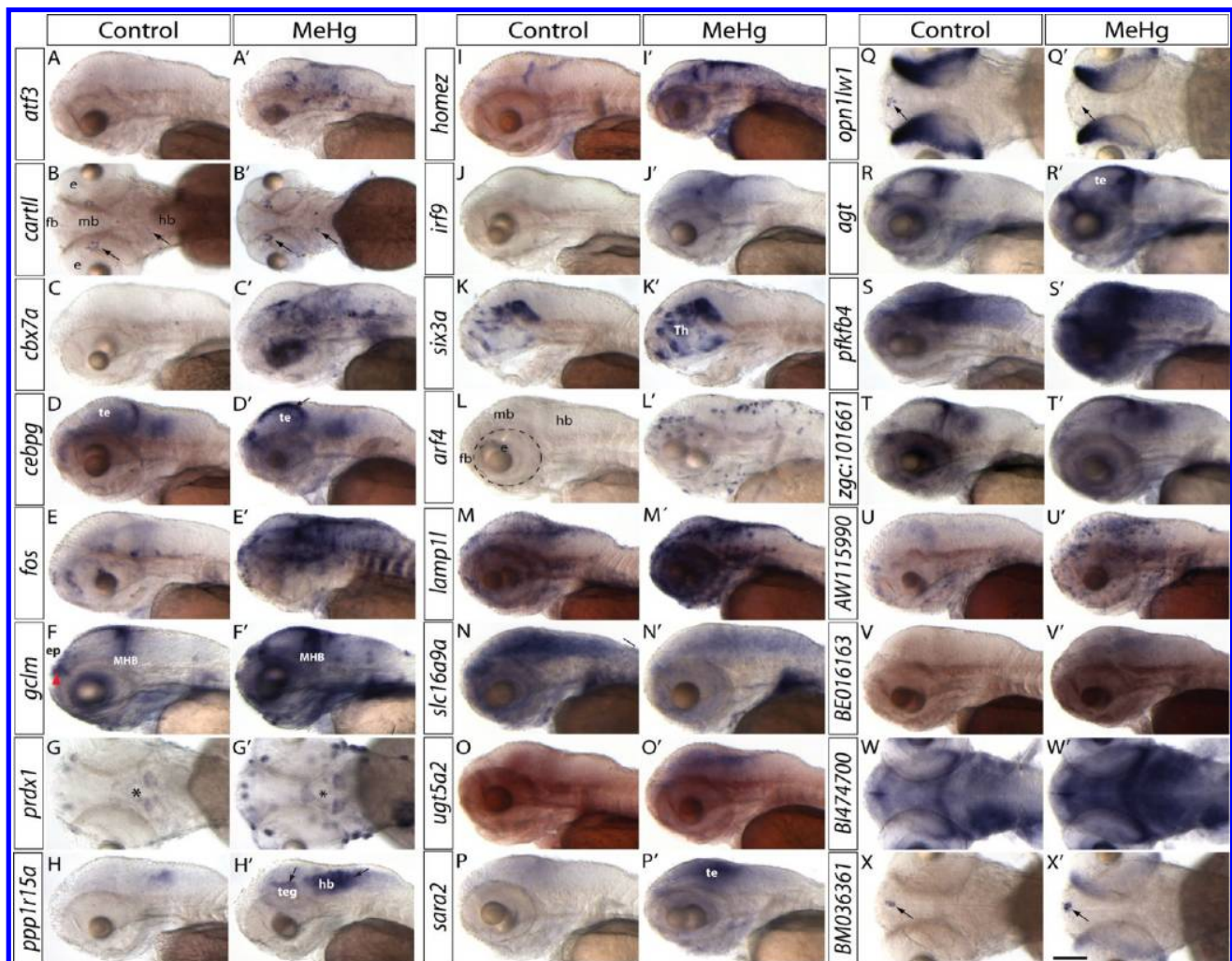


**Figure 4.** Changes in gene expression in the zebra sh brain after MeHg treatment. 72-hpf-old control (A to X) and MeHg-treated (A' to X') embryos performed with in situ hybridization are shown. The dotted line in L indicates the position of the eye; the arrows in Q, Q', X, X' mark the epiphysis. Up-regulations of *atf3* (A, A'), *cartl1* (B, B'), the patches of cells with increased expression are indicated by arrows, *cbx7a* (C, C'), *cebpg* (D, D'), *fos* (E, E'), *gclm* (F, F'), *prdx1* (G, G'), the asterisks indicate the hypothalamus, *ppp1r15a* (H, H'), *homez* (I, I'), *irf9* (J, J'), *six3a* (K, K'), eyes removed for better observation of the expression pattern in the brain, *arf4* (L, L'), *lamp1l* (M, M'), *ugt5a2* (O, O'), *sara2* (P, P'), *agt* (R, R'), *pfkfb4* (S, S'), *zgc:101661* (T, T'), *AW115990* (U, U'), *BE016163* (V, V'), *BI474700* (W, W'), and *BM036361* (X, X'), and down-regulations of *slc16a9a* (N, N') and *opn1lw1* (Q, Q') were observed in the brain of embryos exposed to MeHg. Abbreviations, e, eye; fb, forebrain; hb, hindbrain; mb, midbrain; ep, epiphysis; te, tectum; teg, tegmentum; Th, thalamus; MHB, midbrain-hindbrain boundary. Orientation of embryos: Lateral views with anterior to the left and dorsal side up (A, A', C, C' - F, F', H, H' - P, P', R, R' - V, V'), and dorsal views with anterior to the left and right side up (B, B', G, G', Q, Q', W, W', X, X'). Scale bar, A, A' - F, F', H, H' - P, P', R, R' - V, V', 100  $\mu$ m, G, G', Q, Q', W, W', X, X', 80  $\mu$ m.

The expression of *opsin 1 cone pigment long-wave-sensitive, 1* (*opn1lw1*) was decreased in the epiphysis and in the retina after MeHg exposure (Figure 4Q, Q') suggesting that photoreceptor development is impaired in MeHg-treated embryos. The expression of *angiotensinogen* (*agt*) was slightly increased by MeHg treatment in areas of expression of control embryos such as the boundaries between forebrain/midbrain and midbrain/hindbrain and in the dorsal region of the tectum (Figure 4R, R'). *6-phosphofructo-2-kinase/fructose-2,6-biphosphatase 4-like* (*pfkfb4*) showed an increase in expression in the whole brain after MeHg treatment (Figure 4S, S'). Five other genes with unknown identity (*zgc:101661*, *AW115990*, *BE016163*, *BI474700*, and *BM036361*) were also ectopically expressed in the brain after MeHg exposure (Figure 4T, T' - X, X').

The genes up-regulated in the brain are involved in diverse biological processes and molecular functions, such as tran-

scription regulation (*six3*, *atf3*, *homez*, *fos*, *cbx7a*, *cebpg*, *irf9*), developmental processes (*irf9*, *homez*, *six3a*) oxidative stress (*gclm*, *fos*, *atf3*, *prdx1*, *cebpg*), transport (*arf4*, *lamp1l*, *ugt5a2*, *sara2*, *slc16a9a*), immune response (*atf3*, *cebpg*, *irf9*, *prdx1*) and neuroprotection and cell survival (*cartl1*, *cbx7a*). Although a number of these genes are broadly up-regulated in the brain (*pfkfb4*, *sara2*, *slc16a9a*, *W115990*, *BI474700*, *BE016163*), others show restricted patterns of expression, indicating that they are involved in region-specific responses to MeHg exposure.

## DISCUSSION

In this study, we combined transcriptional profiling of MeHg-exposed embryos with a detailed in situ expression analysis. The aim was to examine tissue-specific effects of MeHg and in particular to identify changes in gene expression, which may

relate to the neurotoxic effect of MeHg. The identified MeHg-regulated genes are involved in various biological processes and molecular functions, such as regulation of transcription, antioxidant defense, immune response, and transport. Altered expression of genes was noted in various organs including the brain, eyes, olfactory bulb, branchial arches, heart, liver, gut, pronephros, somites, lateral lines, pectoral fins, caudal fin fold, blood vessels, skin, YSL pigment cells, and notochord. Many of the examined genes show tissue restricted expression. This indicates (1) that MeHg affects many different tissues in the embryo and (2) that tissues respond with specific gene responses. There were even differences in the response in structures such as the caudal fin and the pectoral fin that are composed of similar cell types and are equally thin and exposed to the MeHg in the water. The expression of some genes was altered in either the pectoral fin (*c6*, *gclm*, *rrad*, *slc16a9a*, *BI474700*) or the caudal fin (*copeb*, *mmp14a*, *sp9*, *p53*, *ucp1*, *AI397362*) in response to MeHg. However, we found also similarities in the gene responses in some tissues. Prominent clustering of coexpression patterns was found in the liver and YSL as well as in the retina and brain. This suggests differences, but also similarities, in the response to MeHg exposure in different tissues. In four cases, we found genes whose expression levels were decreased in some tissues and increased in others. In these cases, the microarray results of whole embryos scored the net change of expression. This underscores again that individual tissues can respond in a very specific manner to MeHg exposure.

From the 88 genes analyzed by in situ hybridization, 24 genes showed specific changes of expression in the brain of zebra sh embryos and are thus prime candidates for genes, which respond to or mediate the neurotoxic effect of MeHg. These genes cover a wide range of biological and molecular functions, including transcription regulation such as *six3*,<sup>74</sup> *atf3*,<sup>75,76</sup> *homez*,<sup>77</sup> *fos*,<sup>78,79</sup> *cbx7a*,<sup>49,80</sup> *cebpg*,<sup>81</sup> and *irf9*,<sup>82</sup> response to oxidative stress such as *gclm*,<sup>83</sup> *fos*,<sup>51,52</sup> and *prdx1*,<sup>84</sup> apoptosis such as *agt*,<sup>85</sup> *atf3*,<sup>53</sup> and *ppp1r15a*,<sup>86</sup> immune response such as *atf3*,<sup>53</sup> *cebpg*,<sup>87</sup> *irf9*,<sup>88</sup> and *prdx1*,<sup>54</sup> cytokine production such as *cebpg*,<sup>89</sup> and *irf9*,<sup>90</sup> and blood vessel regulation such as *agt*,<sup>91,92</sup> and *gclm*.<sup>93</sup> Some of the genes (*pfkfb4l*, *sara2*, *slc16a9a*, *AW115990*, *BI474700*, and *BE016163*) are expressed ubiquitously in the brain, others were restricted in their pattern of expression. This latter observation suggests regionally restricted responses in the brain to MeHg exposure. Given the known molecular interaction of MeHg with cellular processes and molecules such as sulfhydryl groups, the induction of oxidative stress and the disruption of calcium ion homeostasis,<sup>17–24</sup> many cell types should be affected by MeHg. It is thus surprising that quite a number of the genes are induced in a regionally restricted manner in MeHg-exposed embryos. Thus, MeHg seems to affect cells differently leading to cell-specific responses. In addition to regional differences in the gene responses to MeHg exposure, unequal accumulation of MeHg<sup>94,95</sup> may contribute to these differences.

**Comparison with Effects Reported on Adult Zebra-sh.** MeHg has been demonstrated to be hepatotoxic in adult zebra sh, rat and mummichog.<sup>96,32,97</sup> The increase in expression of antioxidant genes in the liver in MeHg-treated zebra sh embryos, such as *prx1*, *gclm*, and *uricase*, indicated that the liver suffered oxidative stress, which may be cause or consequence of hepatocellular damage.<sup>98,85</sup> Since the liver is an organ with a strong innate immunity,<sup>99,100</sup> reactive oxygen

species may be also generated as an inflammatory response to tissue damage. In this context, it may be of relevance that we observed up-regulation of complement components *c3a*, *c4-2*, and *cfb* in the liver in response to MeHg exposure.

In a study by Gonzalez and co-workers,<sup>33</sup> the effect of chronic exposure to MeHg was determined after dietary intake of MeHg for 7, 21, and 63 days. The changes in the expression levels of 13 genes known to be involved in antioxidative defenses, apoptosis, metal chelation, active efflux of organic compounds, mitochondrial metabolism were determined by real-time PCR. Although there were changes in the expression levels of some of the genes examined in the muscle and liver after MeHg exposure, no such changes were observed in the brain. In another study performed by Richter,<sup>31</sup> the acute effect of MeHg exposure on the adult zebra sh brain was investigated by intraperitoneal injection of 0.5  $\mu$ g MeHg/g body weight into female zebra sh. After 96 h, the sh were sacrificed for examination of gene expression levels using a 22K-probe microarray. Seventy-nine genes were shown to be up-regulated and 76 genes were down-regulated ( $p > 0.01$ ) in response to MeHg. In contrast to the study performed by Gonzalez et al., but consistent with our measurements, they detected the up-regulation of oxidative stress and apoptosis genes in the brain after MeHg exposure.

A study of the visual system in adult zebra sh showed that MeHg could pass through the blood-retina barrier and accumulate in various regions of the retina, especially in the photoreceptor layer and in the inner and outer nuclear layer.<sup>34</sup> These observations are consistent with our data in the embryo that showed down-regulation of opsin expression in the developing retina. Taken together, our data derived from zebra sh embryos reflect the MeHg toxicity observed in adult zebra sh.

**How Does MeHg Act As a Neurotoxicant?** It was previously suggested that exposure of embryos to 10, 50, and 80  $\mu$ g/L MeHg decreased cell proliferation in the neural tube.<sup>101</sup> However the authors of this previous study did not observe a dose-dependence, raising concerns whether the observed reduction in cell proliferation was indeed caused by MeHg. When exposing zebra sh embryos from 4 to 72 hpf to 60  $\mu$ g/L MeHg, we did not observe changes in the overall patterning of the brain when probing with a number of developmental regulators (*shha*, *pax6a*, *crestin*, *nurr1*) and genes involved in neurotransmission (*cb1*, *serta*, *TH*). The induction of the developmental regulators *irf9*, *homez*, and *six3a* may thus be related to local repair processes rather than to a disturbance of the overall patterning of the brain. This suggests that the overall patterning of the brain is not significantly affected. The effects of MeHg on the developing nervous system may, however, be too subtle to be detected by overall morphological analysis. Clearly, the heads of MeHg-exposed embryos were smaller. We found increased or ectopic expression of a number of genes whose function is related to oxidative stress, transport and transcription regulation. It is intriguing that some of these genes (*c-fos*, *cebpg*, *atf*, *socs3*) are induced by cAMP in mammalian embryos.<sup>102–106</sup> In light of the view that the cAMP pathway and downstream genes like *c-fos* are involved in learning and memory in mammals,<sup>107,108</sup> it is tempting to speculate that MeHg-induced cellular stress may affect the development and function of the nervous system by aberrantly inducing these regulators of brain function. This disturbance may account for the mental deficits seen in humans exposed during the prenatal period to low doses of MeHg.



## ASSOCIATED CONTENT

## \* Supporting Information

Additional information including tables and figures. This material is available free of charge via the Internet at <http://pubs.acs.org>.

## AUTHOR INFORMATION

## Corresponding Author

\*E-mail: [uwe.straehle@kit.edu](mailto:uwe.straehle@kit.edu).

## Author Contributions

These authors contributed equally to this study.

## Notes

The authors declare no competing financial interest.

## ACKNOWLEDGMENTS

We thank M. Rastegar for help with the microscopes. We are thankful to N. Borel and her team for zebrafish maintenance. We are grateful to X. Cousin, M. Halpern, V. Laudet, A. Fjose, K. Shirabe, and P. Ingham for cDNAs. We acknowledge support by EU IP ZF-Models (LSHG-CT-2003 503496), EUTRACC (LSHG-CT-2006-037445), EU IP ZF-Health Grant (No 242048), BMBF GENDarT2 (AZ:0315190 B) und BMBF DanTox (02WU1053-01).

## REFERENCES

- (1) Ekino, S.; Susa, M.; Ninomiya, T.; Imamura, K.; Kitamura, T. Minamata disease revisited: An update on the acute and chronic manifestations of methyl mercury poisoning. *J. Neurol. Sci.* **2007**, *262* (1–2), 131–44.
- (2) Eto, K.; Marumoto, M.; Takeya, M. The pathology of methylmercury poisoning (Minamata disease). *Neuropathology* **2010**, DOI: 10.1111/j.1440-1789.2010.01119.x.
- (3) Harada, M. Minamata disease: Methylmercury poisoning in Japan caused by environmental pollution. *Crit. Rev. Toxicol.* **1995**, *25* (1), 1–24.
- (4) Sams, C. E. *Methylmercury Contamination: Impacts on Aquatic Systems and Terrestrial Species, and Insights for Abatement*; M. Furniss, C. C., Ronnenberg, K., Ed.; San Diego, CA, 2004.
- (5) Seigneur, C.; Vijayaraghavan, K.; Lohman, K.; Karamchandani, P.; Scott, C. Global source attribution for mercury deposition in the United States. *Environ. Sci. Technol.* **2004**, *38* (2), 555–69.
- (6) USEPA. *National Primary Drinking Water Regulations, Contaminant Specific Fact Sheets, Inorganic Chemicals*, Technical Version; U.S. Environmental Protection Agency: Washington, DC, 1995.
- (7) NJDEP. *Final report on Municipal Solid Waste Incineration*; New Jersey Department of Environmental Protection, 1993.
- (8) Dooley, H. *Natural Sources of Mercury in the Kirkwood-Cohansey Aquifer System of the New Jersey Coastal Plain*; New Jersey Geological Survey, 1992.
- (9) Clarkson, T. W. Mercury: Major issues in environmental health. *Environ. Health Perspect.* **1993**, *100*, 31–8.
- (10) Madenjian, C. P.; O'Connor, D. V. Trophic transfer efficiency of mercury to lake whitefish *Coregonus clupeaformis* from its prey. *Bull. Environ. Contam. Toxicol.* **2008**, *81* (6), 566–70.
- (11) USEPA. *Water Quality Criterion for the Protection of Human Health: Methylmercury*; U. S. Environmental Protection Agency, Office of Science and Technology: Washington, DC, 2001.
- (12) Clarkson, T. W. The three modern faces of mercury. *Environ. Health Perspect.* **2002**, *110* (Suppl 1), 11–23.
- (13) Ask, K.; Akesson, A.; Berglund, M.; Vahter, M. Inorganic mercury and methylmercury in placenta of Swedish women. *Environ. Health Perspect.* **2002**, *110* (5), 523–6.
- (14) Cernichiar, E.; Toribara, T. Y.; Liang, L.; Marsh, D. O.; Berlin, M. W.; Myers, G. J.; Cox, C.; Shamlaye, C. F.; Choisy, O.; Davidson, P.; et al. The biological monitoring of mercury in the Seychelles study. *Neurotoxicology* **1995**, *16* (4), 613–28.
- (15) Grandjean, P.; Weihe, P.; White, R. F.; Debes, F.; Araki, S.; Yokoyama, K.; Murata, K.; Sorensen, N.; Dahl, R.; Jorgensen, P. J. Cognitive deficit in 7-year-old children with prenatal exposure to methylmercury. *Neurotoxicol. Teratol.* **1997**, *19* (6), 417–28.
- (16) Clarkson, T. W.; Magos, L. The toxicology of mercury and its chemical compounds. *Crit. Rev. Toxicol.* **2006**, *36* (8), 609–62.
- (17) Ali, S. F.; LeBel, C. P.; Bondy, S. C. Reactive oxygen species formation as a biomarker of methylmercury and trimethyltin neurotoxicity. *Neurotoxicology* **1992**, *13* (3), 637–48.
- (18) Atchison, W. D. Effects of toxic environmental contaminants on voltage-gated calcium channel function: From past to present. *J. Bioenerg. Biomembr.* **2003**, *35* (6), S07–32.
- (19) Kidd, P. Glutathione: Systemic protectant against oxidative and free radical damage. *Alternate Med. Rev.* **1997**, *2*, 155–176.
- (20) Quig, D. Cysteine metabolism and metal toxicity. *Alternate Med. Rev.* **1998**, *3* (4), 262–70.
- (21) Sarafian, T. A. Methylmercury-induced generation of free radicals: Biological implications. *Met. Ions Biol. Syst.* **1999**, *36*, 415–44.
- (22) Shafer, T. J.; Contreras, M. L.; Atchison, W. D. Characterization of interactions of methylmercury with  $Ca^{2+}$  channels in synaptosomes and pheochromocytoma cells: Radiotracer flux and binding studies. *Mol. Pharmacol.* **1990**, *38* (1), 102–13.
- (23) Shanker, G.; Aschner, J. L.; Syversen, T.; Aschner, M. Free radical formation in cerebral cortical astrocytes in culture induced by methylmercury. *Brain Res. Mol. Brain Res.* **2004**, *128* (1), 48–57.
- (24) Vallee, B. L.; Ulmer, D. D. Biochemical effects of mercury, cadmium, and lead. *Annu. Rev. Biochem.* **1972**, *41* (10), 91–128.
- (25) Samson, J. C.; Shenker, J. The teratogenic effects of methylmercury on early development of the zebrafish, *Danio rerio*. *Aquat. Toxicol.* **2000**, *48* (2–3), 343–354.
- (26) Yang, L.; Kemadjou, J. R.; Zinsmeister, C.; Bauer, M.; Legradi, J.; Muller, F.; Pankratz, M.; Jakel, J.; Strahle, U. Transcriptional profiling reveals barcode-like toxicogenomic responses in the zebrafish embryo. *Genome Biol.* **2007**, *8* (10), R227.
- (27) Yang, L.; Ho, N. Y.; Muller, F.; Strahle, U. Methyl mercury suppresses the formation of the tail primordium in developing zebrafish embryos. *Toxicol. Sci.* **2010**, *115* (2), 379–90.
- (28) Samson, J. C.; Goodridge, R.; Olobatuyi, F.; Weis, J. S. Delayed effects of embryonic exposure of zebrafish (*Danio rerio*) to methylmercury (MeHg). *Aquat. Toxicol.* **2001**, *51* (4), 369–76.
- (29) Cambier, S.; Gonzalez, P.; Durrieu, G.; Maury-Brachet, R.; Boudou, A.; Bourdineaud, J. P. Serial analysis of gene expression in the skeletal muscles of zebrafish fed with a methylmercury-contaminated diet. *Environ. Sci. Technol.* **2010**, *44* (1), 469–75.
- (30) Klaper, R.; Carter, B. J.; Richter, C. A.; Drevnick, P. E.; Sandheinrich, M. B.; Tillitt, D. E. use of a 15k gene microarray to determine gene expression changes in response to acute and chronic methylmercury exposure in the fathead minnow *Pimephales promelas* raginesque. *J. Fish Biol.* **2008**, *72*, 2207–2280.
- (31) Richter, C. A.; Garcia-Reyero, N.; Martyniuk, C.; Knoeb, I.; Pope, M.; Wright-Osment, M. K.; Denslow, N. D.; Tillitt, D. E. Gene expression changes in female zebrafish (*Danio rerio*) brain in response to acute exposure to methylmercury. *Environ. Toxicol. Chem.* **2011**, *30* (2), 301–8.
- (32) Ung, C. Y.; Lam, S. H.; Hlaing, M. M.; Winata, C. L.; Korzh, S.; Mathavan, S.; Gong, Z. Mercury-induced hepatotoxicity in zebrafish: In vivo mechanistic insights from transcriptome analysis, phenotype anchoring and targeted gene expression validation. *BMC Genom.* **2010**, *11*, 212.
- (33) Gonzalez, P.; Dominique, Y.; Massabau, J. C.; Boudou, A.; Bourdineaud, J. P. Comparative effects of dietary methylmercury on gene expression in liver, skeletal muscle, and brain of the zebrafish (*Danio rerio*). *Environ. Sci. Technol.* **2005**, *39* (11), 3972–80.
- (34) Mela, M.; Cambier, S.; Mesmer-Dudons, N.; Legeay, A.; Grotzner, S. R.; de Oliveira Ribeiro, C. A.; Ventura, D. F.; Massabau, J. C. Methylmercury localization in *Danio rerio* retina after trophic and subchronic exposure: a basis for neurotoxicology. *Neurotoxicology* **2010**, *31* (5), 448–53.

- (35) Mikut, R. B.; Braun, O.; S. Reischl, M., The open source MATLAB toolbox Gait-CAD and its application to bioelectric signal processing. In *In Proc., DGBMT-Workshop Biosignalverarbeitung*; Potsdam, 2008; pp pp109–111.
- (36) Simon, R. M. K.; McShane, E. L.; Radmacher, L. M.; Wright, M. D.; G. W. Zhao, Y. *Design and Analysis of DNA Microarray Investigation*; Springer, 2004.
- (37) Kupersmidt, I.; Su, Q. J.; Grewal, A.; Sundaresh, S.; Halperin, I.; Flynn, J.; Shekar, M.; Wang, H.; Park, J.; Cui, W.; Wall, G. D.; Wisotzkey, R.; Alag, S.; Akhtari, S.; Ronaghi, M., Ontology-based meta-analysis of global collections of high-throughput public data. *PLoS One* **2010**, *5* (9).
- (38) Durinck, S.; Moreau, Y.; Kasprzyk, A.; Davis, S.; De Moor, B.; Brazma, A.; Huber, W. BioMart and bioconductor: A powerful link between biological databases and microarray data analysis. *Bioinformatics* **2005**, *21* (16), 3439–40.
- (39) Zhang, B.; Kirov, S.; Snoddy, J. WebGestalt: An integrated system for exploring gene sets in various biological contexts. *Nucleic Acids Res.* **2005**, *33* (Web Server issue), W741–8.
- (40) Duncan, D. T.; Prodduturi, N.; Zhang, B. WebGestalt2: An updated and expanded version of the web-based gene set analysis toolkit. *BMC Bioinf.* **2010**, *11* (supple 4), P10.
- (41) Oxtoby, E.; Jowett, T. Cloning of the zebrafish krox-20 gene (krx-20) and its expression during hindbrain development. *Nucleic Acids Res.* **1993**, *21* (5), 1087–95.
- (42) Wester eld, M. *The Zebra sh Book a Guide for the Laboratory Use of Zebra sh (Danio rerio)*; University of Oregon: Eugene, 2000; Vol. 4.
- (43) de Hoon, M. J.; Imoto, S.; Nolan, J.; Miyano, S. Open source clustering software. *Bioinformatics* **2004**, *20* (9), 1453–4.
- (44) Chen, B. P.; Wolfgang, C. D.; Hai, T. Analysis of ATF3, a transcription factor induced by physiological stresses and modulated by gadd153/Chop10. *Mol. Cell. Biol.* **1996**, *16* (3), 1157–68.
- (45) Zhang, S. J.; Buchthal, B.; Lau, D.; Hayer, S.; Dick, O.; Schwaninger, M.; Veltkamp, R.; Zou, M.; Weiss, U.; Bading, H. A signaling cascade of nuclear calcium-CREB-ATF3 activated by synaptic NMDA receptors defines a gene repression module that protects against extrasynaptic NMDA receptor-induced neuronal cell death and ischemic brain damage. *J. Neurosci.* **2011**, *31* (13), 4978–90.
- (46) Jia, J.; Chen, X.; Zhu, W.; Luo, Y.; Hua, Z.; Xu, Y. CART protects brain from damage through ERK activation in ischemic stroke. *Neuropeptides* **2008**, *42* (5–6), 653–61.
- (47) Mao, P.; Ardeshtiri, A.; Jacks, R.; Yang, S.; Hurn, P. D.; Alkayed, N. J. Mitochondrial mechanism of neuroprotection by CART. *Eur. J. Neurosci.* **2007**, *26* (3), 624–32.
- (48) Xu, Y.; Zhang, W.; Klaus, J.; Young, J.; Koerner, I.; Sheldahl, L. C.; Hurn, P. D.; Martinez-Murillo, F.; Alkayed, N. J. Role of cocaine- and amphetamine-regulated transcript in estradiol-mediated neuroprotection. *Proc. Natl. Acad. Sci. U. S. A.* **2006**, *103* (39), 14489–94.
- (49) Gil, J.; Bernard, D.; Martinez, D.; Beach, D. Polycomb CBX7 has a unifying role in cellular lifespan. *Nat. Cell Biol.* **2004**, *6* (1), 67–72.
- (50) Mullins, D. N.; Crawford, E. L.; Khuder, S. A.; Hernandez, D. A.; Yoon, Y.; Willey, J. C. CEBPG transcription factor correlates with antioxidant and DNA repair genes in normal bronchial epithelial cells but not in individuals with bronchogenic carcinoma. *BMC Cancer* **2005**, *5*, 141.
- (51) Rao, G. N.; Glasgow, W. C.; Eling, T. E.; Runge, M. S. Role of hydroperoxyeicosatetraenoic acids in oxidative stress-induced activating protein 1 (AP-1) activity. *J. Biol. Chem.* **1996**, *271* (44), 27760–4.
- (52) Tormos, C.; Javier Chaves, F.; Garcia, M. J.; Garrido, F.; Jover, R.; O'Connor, J. E.; Iradi, A.; Oltra, A.; Oliva, M. R.; Saez, G. T. Role of glutathione in the induction of apoptosis and c-fos and c-jun mRNAs by oxidative stress in tumor cells. *Cancer Lett.* **2004**, *208* (1), 103–13.
- (53) Thompson, M. R.; Xu, D.; Williams, B. R. ATF3 transcription factor and its emerging roles in immunity and cancer. *J. Mol. Med. (Berlin)* **2009**, *87* (11), 1053–60.
- (54) Geiben-Lynn, R.; Kursar, M.; Brown, N. V.; Addo, M. M.; Shau, H.; Lieberman, J.; Luster, A. D.; Walker, B. D. HIV-1 antiviral activity of recombinant natural killer cell enhancing factors, NKEF-A and NKEF-B, members of the peroxiredoxin family. *J. Biol. Chem.* **2003**, *278* (3), 1569–74.
- (55) Scott, D. W.; Mutamba, S.; Hopkins, R. G.; Loo, G. Increased GADD gene expression in human colon epithelial cells exposed to deoxycholate. *J. Cell Physiol.* **2005**, *202* (1), 295–303.
- (56) Ghimouz, R.; Bar, I.; Hanotel, J.; Minela, B.; Keruzore, M.; Thelie, A.; Bellefroid, E. J. The homeobox leucine zipper gene Homez plays a role in *Xenopus laevis* neurogenesis. *Biochem. Biophys. Res. Commun.* **2011**, *415* (1), 11–6.
- (57) Krauss, S.; Concorde, J. P.; Ingham, P. W. A functionally conserved homolog of the *Drosophila* segment polarity gene hh is expressed in tissues with polarizing activity in zebrafish embryos. *Cell* **1993**, *75* (7), 1431–44.
- (58) Krauss, S.; Johansen, T.; Korzh, V.; Fjose, A. Expression pattern of zebrafish pax genes suggests a role in early brain regionalization. *Nature* **1991**, *353* (6341), 267–70.
- (59) Nikaïdo, M.; Tada, M.; Saji, T.; Ueno, N. Conservation of BMP signaling in zebrafish mesoderm patterning. *Mech. Dev.* **1997**, *61* (1–2), 75–88.
- (60) Kiefer, P.; Strahle, U.; Dickson, C. The zebrafish Fgf-3 gene: cDNA sequence, transcript structure and genomic organization. *Gene* **1996**, *168* (2), 211–5.
- (61) Maroon, H.; Walshe, J.; Mahmood, R.; Kiefer, P.; Dickson, C.; Mason, I. Fgf3 and Fgf8 are required together for formation of the otic placode and vesicle. *Development* **2002**, *129* (9), 2099–108.
- (62) Kelly, G. M.; Moon, R. T. Involvement of wnt1 and pax2 in the formation of the midbrain-hindbrain boundary in the zebrafish gastrula. *Dev. Genet.* **1995**, *17* (2), 129–40.
- (63) Lam, C. S.; Marz, M.; Strahle, U. Gfap and nestin reporter lines reveal characteristics of neural progenitors in the adult zebrafish brain. *Dev. Dyn.* **2009**, *238* (2), 475–86.
- (64) Blader, P.; Strahle, U.; Ingham, P. W. Three Wnt genes expressed in a wide variety of tissues during development of the zebrafish, *Danio rerio*: Developmental and evolutionary perspectives. *Dev. Genes Evol.* **1996**, *206* (1), 3–13.
- (65) Rubinstein, A. L.; Lee, D.; Luo, R.; Henion, P. D.; Halpern, M. E. Genes dependent on zebrafish cyclops function identified by AFLP differential gene expression screen. *Genesis* **2000**, *26* (1), 86–97.
- (66) Bertrand, C.; Chatonnet, A.; Takke, C.; Yan, Y. L.; Postlethwait, J.; Toutant, J. P.; Cousin, X. Zebrafish acetylcholinesterase is encoded by a single gene localized on linkage group 7. Gene structure and polymorphism; molecular forms and expression pattern during development. *J. Biol. Chem.* **2001**, *276* (1), 464–74.
- (67) Lam, C. S.; Rastegar, S.; Strahle, U. Distribution of cannabinoid receptor 1 in the CNS of zebrafish. *Neuroscience* **2006**, *138* (1), 83–95.
- (68) Wang, Y.; Takai, R.; Yoshioka, H.; Shirabe, K. Characterization and expression of serotonin transporter genes in zebrafish. *Tohoku J. Exp. Med.* **2006**, *208* (3), 267–74.
- (69) Escriva, H.; Safi, R.; Hanni, C.; Langlois, M. C.; Saumitou-Laprade, P.; Stehelin, D.; Capron, A.; Pierce, R.; Laudet, V. Ligand binding was acquired during evolution of nuclear receptors. *Proc. Natl. Acad. Sci. U. S. A.* **1997**, *94* (13), 6803–8.
- (70) Wullimann, M. F.; Rink, E. Detailed immunohistochemistry of Pax6 protein and tyrosine hydroxylase in the early zebrafish brain suggests role of Pax6 gene in development of dopaminergic diencephalic neurons. *Brain Res. Dev. Brain Res.* **2001**, *131* (1–2), 173–91.
- (71) Donaldson, J. G.; Honda, A. Localization and function of Arf family GTPases. *Biochem. Soc. Trans.* **2005**, *33* (Pt 4), 639–42.
- (72) King, C. D.; Rios, G. R.; Green, M. D.; Tephly, T. R. UDP-glucuronosyltransferases. *Curr. Drug Metab.* **2000**, *1* (2), 143–61.
- (73) Jones, B.; Jones, E. L.; Bonney, S. A.; Patel, H. N.; Mensenkamp, A. R.; Eichenbaum-Voline, S.; Rudling, M.; Myrdal, U.; Annesi, G.; Naik, S.; Meadows, N.; Quattrone, A.; Islam, S. A.; Naoumova, R. P.; Angelin, B.; Infante, R.; Levy, E.; Roy, C. C.; Freemont, P. S.; Scott, J.; Shoulders, C. C. Mutations in a Sar1 GTPase of COPII vesicles are

associated with lipid absorption disorders. *Nat. Genet.* **2003**, *34* (1), 29–31.

(74) Kobayashi, M.; Toyama, R.; Takeda, H.; Dawid, I. B.; Kawakami, K. Overexpression of the forebrain-specific homeobox gene *six3* induces rostral forebrain enlargement in zebrafish. *Development* **1998**, *125* (15), 2973–82.

(75) Hsu, J. C.; Laz, T.; Mohn, K. L.; Taub, R. Identification of LRF-1, a leucine-zipper protein that is rapidly and highly induced in regenerating liver. *Proc. Natl. Acad. Sci. U. S. A.* **1991**, *88* (9), 3511–5.

(76) Chu, H. M.; Tan, Y.; Kobierski, L. A.; Balsam, L. B.; Comb, M. J. Activating transcription factor-3 stimulates 3',5'-cyclic adenosine monophosphate-dependent gene expression. *Mol. Endocrinol.* **1994**, *8* (1), 59–68.

(77) Bayarsaihan, D.; Enkhmandakh, B.; Makeyev, A.; Grealley, J. M.; Leckman, J. F.; Ruddle, F. H. Homez, a homeobox leucine zipper gene specific to the vertebrate lineage. *Proc. Natl. Acad. Sci. U. S. A.* **2003**, *100* (18), 10358–63.

(78) Curran, T.; Morgan, J. I. Fos: An immediate-early transcription factor in neurons. *J. Neurobiol.* **1995**, *26* (3), 403–12.

(79) Kovacs, K. J. c-Fos as a transcription factor: A stressful (re)view from a functional map. *Neurochem. Int.* **1998**, *33* (4), 287–97.

(80) Li, Q.; Wang, X.; Lu, Z.; Zhang, B.; Guan, Z.; Liu, Z.; Zhong, Q.; Gu, L.; Zhou, J.; Zhu, B.; Ji, J.; Deng, D. Polycomb CBX7 directly controls trimethylation of histone H3 at lysine 9 at the p16 locus. *PLoS One* **2010**, *5* (10), e13732.

(81) Davydov, I. V.; Bohmann, D.; Krammer, P. H.; Li-Weber, M. Cloning of the cDNA encoding human C/EBP gamma, a protein binding to the PRE-I enhancer element of the human interleukin-4 promoter. *Gene* **1995**, *161* (2), 271–5.

(82) Veals, S. A.; Santa Maria, T.; Levy, D. E. Two domains of ISGF3 gamma that mediate protein-DNA and protein-protein interactions during transcription factor assembly contribute to DNA-binding specificity. *Mol. Cell. Biol.* **1993**, *13* (1), 196–206.

(83) Lu, S. C. Regulation of glutathione synthesis. *Mol. Aspects Med.* **2009**, *30* (1–2), 42–59.

(84) Immenschuh, S.; Baumgart-Vogt, E. Peroxiredoxins, oxidative stress, and cell proliferation. *Antioxid. Redox Signaling* **2005**, *7* (5–6), 768–77.

(85) Liu, Y.; Wang, J.; Wei, Y.; Zhang, H.; Xu, M.; Dai, J. Induction of time-dependent oxidative stress and related transcriptional effects of perfluorododecanoic acid in zebrafish liver. *Aquat. Toxicol.* **2008**, *89* (4), 242–50.

(86) Hollander, M. C.; Poola-Kella, S.; Fornace, A. J., Jr. Gadd34 functional domains involved in growth suppression and apoptosis. *Oncogene* **2003**, *22* (25), 3827–32.

(87) Hutton, J. J.; Jegga, A. G.; Kong, S.; Gupta, A.; Ebert, C.; Williams, S.; Katz, J. D.; Aronow, B. J. Microarray and comparative genomics-based identification of genes and gene regulatory regions of the mouse immune system. *BMC Genom.* **2004**, *5*, 82.

(88) Taniguchi, T.; Ogasawara, K.; Takaoka, A.; Tanaka, N. IRF family of transcription factors as regulators of host defense. *Annu. Rev. Immunol.* **2001**, *19*, 623–55.

(89) Gao, H.; Parkin, S.; Johnson, P. F.; Schwartz, R. C. C/EBP gamma has a stimulatory role on the IL-6 and IL-8 promoters. *J. Biol. Chem.* **2002**, *277* (41), 38827–37.

(90) Nguyen, H.; Hiscott, J.; Pitha, P. M. The growing family of interferon regulatory factors. *Cytokine Growth Factor Rev.* **1997**, *8* (4), 293–312.

(91) Brand, M.; Lamande, N.; Sigmund, C. D.; Larger, E.; Corvol, P.; Gasc, J. M. Angiotensinogen modulates renal vasculature growth. *Hypertension* **2006**, *47* (6), 1067–74.

(92) Nagata, M.; Tanimoto, K.; Fukamizu, A.; Kon, Y.; Sugiyama, F.; Yagami, K.; Murakami, K.; Watanabe, T. Nephrogenesis and renovascular development in angiotensinogen-deficient mice. *Lab. Invest.* **1996**, *75* (5), 745–53.

(93) Nakamura, S.; Sugiyama, S.; Fujioka, D.; Kawabata, K.; Ogawa, H.; Kugiyama, K. Polymorphism in glutamate-cysteine ligase modifier subunit gene is associated with impairment of nitric oxide-mediated coronary vasomotor function. *Circulation* **2003**, *108* (12), 1425–7.

(94) Korbass, M.; Blechinger, S. R.; Krone, P. H.; Pickering, I. J.; George, G. N. Localizing organomercury uptake and accumulation in zebrafish larvae at the tissue and cellular level. *Proc. Natl. Acad. Sci. U. S. A.* **2008**, *105* (34), 12108–12.

(95) Korbass, M.; Krone, P. H.; Pickering, I. J.; George, G. N. Dynamic accumulation and redistribution of methylmercury in the lens of developing zebrafish embryos and larvae. *J. Biol. Inorg. Chem.* **2010**, *15* (7), 1137–45.

(96) Lin, T. H.; Huang, Y. L.; Huang, S. F. Lipid peroxidation in liver of rats administered with methylmercuric chloride. *Biol. Trace Elem. Res.* **1996**, *54*, 33–41.

(97) Weis, P.; Bogden, J. D.; Enslee, E. C. Hg- and Cu-induced hepatocellular changes in the mummichog, *Fundulus heteroclitus*. *Environ. Health Perspect.* **1986**, *65*, 167–173.

(98) Jaeschke, H.; Gores, G. J.; Cederbaum, A. I.; Hinson, J. A.; Pessayre, D.; Lemasters, J. J. Mechanisms of hepatotoxicity. *Toxicol. Sci.* **2002**, *65* (2), 166–76.

(99) Gao, B.; Jeong, W. I.; Tian, Z. Liver: An organ with predominant innate immunity. *Hepatology* **2008**, *47* (2), 729–36.

(100) Racanelli, V.; Rehmann, B. The liver as an immunological organ. *Hepatology* **2006**, *43* (2 Suppl 1), S54–62.

(101) Hassan, S. A.; Moussa, E. A.; Abbott, L. C. The effect of methylmercury exposure on early central nervous system development in the zebrafish (*Danio rerio*) embryo. *J. Appl. Toxicol.* **2011**, *32*, 707–713.

(102) Hart, I. R.; Rao, J.; Wilson, R. E. c-AMP-induced c-fos expression in cells of melanocyte origin. *Biochem. Biophys. Res. Commun.* **1989**, *159* (2), 408–13.

(103) Mehmet, H.; Sinnett-Smith, J.; Moore, J. P.; Evan, G. I.; Rozengurt, E. Differential induction of c-fos and c-myc by cyclic AMP in Swiss 3T3 cells: Significance for the mitogenic response. *Oncogene Res.* **1988**, *3* (3), 281–6.

(104) Milne, G. R.; Palmer, T. M.; Yarwood, S. J. Novel control of cAMP-regulated transcription in vascular endothelial cells. *Biochem. Soc. Trans.* **2012**, *40* (1), 1–5.

(105) Sands, W. A.; Woolson, H. D.; Milne, G. R.; Rutherford, C.; Palmer, T. M. Exchange protein activated by cyclic AMP (Epac)-mediated induction of suppressor of cytokine signaling 3 (SOCS-3) in vascular endothelial cells. *Mol. Cell. Biol.* **2006**, *26* (17), 6333–46.

(106) Yarwood, S. J.; Borland, G.; Sands, W. A.; Palmer, T. M. Identification of CCAAT/enhancer-binding proteins as exchange protein activated by cAMP-activated transcription factors that mediate the induction of the SOCS-3 gene. *J. Biol. Chem.* **2008**, *283* (11), 6843–53.

(107) Countryman, R. A.; Kaban, N. L.; Colombo, P. J. Hippocampal c-fos is necessary for long-term memory of a socially transmitted food preference. *Neurobiol. Learn. Mem.* **2005**, *84* (3), 175–83.

(108) He, J.; Yamada, K.; Nabeshima, T. A role of Fos expression in the CA3 region of the hippocampus in spatial memory formation in rats. *Neuropsychopharmacology* **2002**, *26* (2), 259–68.